

Effect of a Blocked Channel on the Wall Temperature of a Regeneratively Cooled Rocket Thrust Chamber

Mohammad H. Naraghi
Department of Mechanical Engineering, Manhattan College, Riverdale NY 10471,
E-mail: mnaraghi@manhattan.edu

Richard J. Quentmeyer
2703 Country Club Blvd., Rocky River, OH 44116, E-mail: QTyme@msn.com

David H. Mohr
D&E Propulsion & Power Systems, 3840 Hammock Rd, Mims, FL 32754, E-mail: Dave@digital.net

ABSTRACT

This paper presents the effects of a blocked cooling channel on the wall temperature profile for three regeneratively cooled rocket thrust chambers. The Rocket Thermal Evaluation (RTE) code, used for analyzing chamber designs, was modified to model a blocked channel condition. The evaluation results are presented for a relatively low chamber pressure case and two relatively high chamber pressure cases. All three chambers incorporate high-aspect-ratio cooling channels (HARCC) in the designs. The results show that there are additional peak temperature points along the nozzle when a cooling channel is blocked. One peak temperature is in the throat region, similar to that of a chamber having no blocked channels, and another peak temperature point is at the injector end. Also, it is shown that local peak temperature points before and after cooling channel step changes in the nozzle and chamber respectively can be of the same order of magnitude as the maximum wall temperature in the throat region. Although the inclusion of two or more channels adjacent to the blocked channel would further reduce the wall temperature in the blocked channel region, the present analysis only includes the blocked channel and the adjacent open channel, which represents the worst case scenario.

INTRODUCTION

The design of a regeneratively cooled rocket thrust chamber involves a trade-off between obtaining the lowest possible hot-gas-side wall temperature to insure structural integrity and long life of the chamber liner (cooling jacket) and minimizing the

coolant pressure drop to reduce the propellant pumping power. Since the liner of most current rocket thrust chambers is fabricated from a high conductivity material, such as copper, or a copper-based alloy, it is essential that the design, or evaluation, program contain a two- or three-dimensional conduction analysis. This is required in order to make a reasonably accurate prediction of the hot-gas-side wall temperature and the temperature profile within the liner ribs. One of the computer programs used for this type of analysis is RTE [1], which is a rocket thrust chamber thermal evaluation computer program. It combines convection, conduction and radiation heat transfer methodologies coupled to a boundary layer program. The program calculates the local heat flux, wall temperature profiles, coolant temperature rise, pressure drop, Mach number, etc. for a given cooling jacket geometry.

One of the concerns of the rocket designer is what happens to the wall temperature if one of the cooling channels is blocked. Due to symmetry of all of the cooling channels at a given station, it is customary to represent the heat transfer model by one-half of a cooling channel (a half-rib) in cross-section, similar to that shown in Figure 1a. In order to perform a thermal analysis for a chamber liner that has a blocked channel, the heat transfer model in RTE had to be changed. The model is represented by two half-channels (a full-rib), one side representing a channel that is blocked in which there is no convective cooling, while the other side represents the adjacent open channel with coolant flowing in it (see Figure 1b).

In order to show the effects of a blocked cooling channel on the wall temperature profile, three

different rocket thrust chambers were chosen for the analysis. One chamber was designed to operate at a relatively low chamber pressure ($P_c=450$ psia), while the other two chambers were designed to operate at a relatively high chamber pressure ($P_c=2000$ psia). The high pressure chambers used in this analysis are modified designs of the high-pressure chamber designed and tested at the NASA-Glenn Research Center [2, 3]. The liners for all three chambers are made of copper, closed out with nickel, incorporating high- aspect-ratio cooling channels (HARCC) in their designs.

DESCRIPTION OF RTE

Rocket Thermal Evaluation (RTE) [1] is a computer program for thermal analysis of regeneratively cooled rocket engines. RTE has three main modules, hot-gas-side, wall conduction, and coolant modules. For the numerical procedure, the rocket thrust chamber is subdivided into a number of stations along the longitudinal direction. The high-pressure rocket thrust chamber contour is shown in Figure 2 with the station locations denoted on the contour. The thermodynamic and transport properties of the combustion gases in the hot-gas-side module of RTE are evaluated using the chemical equilibrium composition computer program developed by Gordon and McBride [4-5] (CET, Chemical Equilibrium with Transport properties). The GASP (GAS Properties) [6] or WASP (Water And Steam Properties) [7] programs are implemented to obtain coolant thermodynamic and transport properties. Since the heat transfer coefficients of the hot-gas and coolant sides are related to surface temperatures, an iterative procedure is used to evaluate heat transfer coefficients and adiabatic wall temperatures.

The temperature distribution within the wall is determined via a three-dimensional finite difference scheme. In this conduction module, finite difference grids are superimposed on half-rib cells throughout the wall at different stations. The temperature of each node is then written in terms of temperatures of neighboring nodes (the four closest nodes at the same station and two nodes at the neighboring stations). The program marches axially from one station to another. At each station the Gauss-Siedel iterative method in the RTE's conduction module is used to obtain convergence for the temperature distribution along the radial and circumferential directions. With the new blocked channel option, the finite difference grids are superimposed on cells corresponding to full-rib and two half-rib channels (one of channels is fully blocked and the other one is fully open).

The hot-gas-side heat flux calculation for RTE is based on a heat transfer correlation and an adiabatic wall temperature for rapidly accelerating flow (see [8-9] for details). To obtain a better estimate of the hot-gas heat flux RTE is linked to the Boundary Layer Module (BLM) of TDK [10]. A shell program has been developed to interface RTE and TDK. In this shell program RTE's internal heat flux calculation (based on correlations given in [8-9]) is first used to predict wall temperature distributions. Then the calculated wall temperature, via RTE and the TDK interface program (TDK RTE.f), is inserted into the input of TDK. Then by running TDK (with one of its boundary layer modules, BLM or MABL) the wall heat flux based on TDK's boundary layer module is calculated. The heat fluxes for each station are then inserted into the input file of RTE via an interface program (RTE_TDK.f). This cycle is repeated several times until convergence is achieved. At each iterative cycle heat fluxes at all stations are compared to those of previous iteration. This iterative calculation stops when the differences between wall heat fluxes of two consecutive iterations become negligibly small. The flow chart of this iterative scheme is given in Figure 3.

The cooling channel flow model and heat transfer formulation is based on a bulk temperature assumption and use of heat transfer coefficients given in [11-12]. The heat transfer coefficients are evaluated based on temperatures of nodal points at the bottom, side and top walls of cooling channels. The overall heat flux to the coolant at each station is matched to those of conduction through the wall and convection from the hot-gases using an iterative scheme.

It is recognized that there has been a considerable amount of experimental and analysis work done in the area of HARCC, including attempts to show the effects of secondary flow in the channels and striations in the local coolant temperature within the channels [13-17]. However, it is felt that this technology is not yet mature enough to warrant a change in the current coolant side methodology used for the analysis in this paper.

ANALYSIS METHODOLOGY

If one of the cooling channels in a rocket thrust chamber liner is blocked, obviously, the resulting wall temperature of the blocked channel will be higher than that of the cooled channels. However, the channel adjacent to the blocked channel will also have a higher wall temperature than the channels further away from the blocked-channel region due to

conduction of heat from the blocked channel to the adjacent channel. This has the effect of reducing the maximum wall temperature in the blocked channel for a liner made of a high conductivity material. As a result, this causes the coolant temperature in the channel adjacent to the blocked channel to rise to a level higher than that for the channels further away from the blocked channel region. This would result in an increase in coolant Mach number and pressure drop in the adjacent channel, assuming the coolant mass flow in that channel is the same as all of the other channels. However, the pressure drop across the cooling jacket must be equal for all channels. Since the pressure drop across the channel adjacent to the blocked channel must be the same as that of the other channels, the mass flow in that channel will become less than that of the other channels. Therefore, in order to calculate the hot-gas-side wall temperature of the blocked channel and the adjacent channel, the mass flow in the adjacent channel must be determined.

To obtain the mass flow in the cooling channel adjacent to the blocked channel, RTE was first run for a given cooling jacket geometry in which there is no blocked channel in order to determine the pressure drop across the cooling jacket. Then, another case was run using the full-rib conduction model in order to obtain the temperature profile in the rib with no cooling on one side and coolant flowing on the other side (see figure 1b). The mass flow in the adjacent channel is reduced through an iterative scheme until the pressure drop matches that for the case with no blocked channel. Through this procedure the wall temperature and the temperature profile in the blocked channel and the adjacent channel can be calculated.

Although the inclusion of two, or more channels away from the blocked channel in the analysis would further reduce the wall temperature in the blocked channel region, this analysis only includes the blocked channel and the adjacent channel, which represents the worst case scenario.

RESULTS AND DISCUSSION

In order to show effects of a blocked channel on the wall temperature and coolant flow in an adjacent cooling channel of typical regeneratively cooled rocket thrust chambers, three cases were evaluated. The first case is for a low chamber pressure design and the other two cases are for a high chamber pressure design.

Low-pressure Chamber

Chamber pressure	450 psia
O/F	5.8
Contraction ratio	3.07
Expansion ratio	5.3
Throat diameter	8.0 inches
Propellants	GH2-LO2
Coolant	LH2
Total coolant flow rate	15 lb/sec
Coolant inlet temperature	50R
Coolant inlet stagnation pressure	700 psia
Approximate throat heat flux	19 Btu/in ² -sec
Number of cooling channels	240
Throat region channel aspect ratio	5
Channel width step changes at	X=3.039 inches X=-4.158 inches

First, temperature profiles at all stations with all channels open are obtained by running RTE for an unblocked-channel case. The coolant stagnation pressure at the exit of the cooling channel for this case is 507 psia, which results in a pressure drop of 193 psi in the cooling jacket. The highest wall temperature for this engine occurs just upstream of the throat, as expected. Figure 4 shows the rib temperature profile at this location (x=-0.618 inches). As shown in this figure the maximum temperature reaches 723R. Step changes in wall temperature also occur just before and just after the step change in the cooling channel width in the nozzle and chamber respectively.

The same chamber was evaluated by running RTE with the one-blocked-channel option. In this case the channel adjacent to the blocked channel, in addition to its own heat load, will receive the heating load of the blocked channel through conduction. The increased thermal load to the cooling channel adjacent to the blocked channel would result in an increase in pressure drop for that channel. However, since the pressure drop across that channel must be essentially equal to all the other channels, the flow rate in the cooling channel adjacent to the blocked channel is reduced until its pressure drop becomes equal to that for the unblocked-channel case. In this case, the coolant flow rate in the channel adjacent to the blocked channel becomes 0.036 lb/sec, which resulted in a pressure drop of 193 psi, the same pressure drop as the unblocked-channel case. It should be noted that the flow rate per channel for the unblocked-channel case is 0.0625 lb/sec. Thus, the weight flow in the channel adjacent to the blocked channel had to be reduced approximately 42% in order to match the pressure drop of the unblocked-channel case.

The resulting axial average wall temperature profile for the blocked-channel and the adjacent open channel is shown in Figure 5 for the low-pressure chamber. Also shown is the axial average hot-gas-side wall temperature for the same chamber having no blocked channel. When all channels are open the highest wall temperatures for this design occur just upstream of the throat and at $x \approx -4.0$ inches, just after the step change in the cooling channel width. However, for the blocked-channel case, the wall temperature increases significantly in the nozzle and injector-end locations due to the larger mass of material that has to be cooled by the reduction in mass flow in the adjacent channel. A peak wall temperature of 1223R occurs approximately 6.0 inches downstream of the throat, two stations before the step change in the cooling channel width. One of the factors affecting the high wall temperature at this location in the nozzle is the result of a minimum coolant-side heat transfer coefficient occurring at this location due to the coolant transport properties for the local temperature and pressure condition. Figures 6 and 7 show rib temperature profiles at the other peak temperature locations, upstream of the throat and at the injector end of the chamber. Although there is a significant increase in the hot-gas-side wall temperature, the temperatures are not at a catastrophic level for this low chamber pressure case.

To investigate the effect of a blocked channel on the hot-gas-side wall temperature and coolant flow rate in the channel adjacent to a blocked channel for a high chamber pressure condition, two thrust chambers operating at a chamber pressure of 2000 psia were evaluated. Although both chambers incorporate HARCC in their designs, there are different numbers of cooling channels.

High-pressure Chambers

Chamber pressure	2000 psia	2000 psia
O/F	5.8	5.8
Contraction ratio	3.41	3.41
Expansion ratio	6.63	6.63
Throat diameter	2.6 inches	2.6 inches
Propellant	GH2-LO2	GH2-LO2
Coolant	LH2	LH2
Total coolant flow rate	6.45 lb/sec	6.45 lb/sec
Coolant inlet temperature	50	50R
Coolant inlet stagnation pressure	3200 psia	2900 psia
Approximate throat heat flux	$77 \frac{Btu}{in^2 - sec}$	$75 \frac{Btu}{in^2 - sec}$
Number of cooling channels	200	150

Throat region channel aspect ratio	5-7.8	6
Channel width		
step changes at	X=0.947 inches	X=0.947 inches
	X=-3.906 inches	X=-3.906 inches

Similar to the low-pressure chamber, first the temperature profiles at all stations with all channels open are obtained. The 200 channel chamber was evaluated first. In order to allow for the pressure drop across the injector, the coolant inlet pressure required was 3200 psia, resulting in a pressure drop of 834 psi in the cooling jacket, which is relatively high for this chamber pressure. However, the wall temperature just upstream of the throat is only 1058R, which is relatively low for a high-pressure chamber, showing the effectiveness of HARCC in this design. The temperature profile for this location is given in Figure 8. The dashed line in Figure 9 shows the average hot-gas-side wall temperature as a function of axial position for the unblocked-channel case. This figure also shows that there are step changes in the wall temperature, just before and just after step changes in the cooling channel width in the nozzle and chamber respectively, at $x \approx 1.0$ inches and $x \approx -4.0$ inches.

The same high-pressure chamber was evaluated by running RTE with the blocked-channel option. In order to maintain the pressure drop of 834 psi for the cooling channel adjacent to the blocked channel the mass flow rate of the coolant was reduced to 0.024 lb/sec. compared to 0.032 lb/sec per channel for the no-blocked channel case, a 25% drop in the coolant mass flow. The resulting axial average wall temperature profile for the blocked-channel and the adjacent open channel is shown in Figure 9. As shown in this Figure, the maximum wall temperature occurs at the injector-end of the cooling channels. Another location of high temperature occurs at $x \approx -4.0$ inches, where there is a step change in the cooling channel width. Figures 10 and 11 show the rib temperature profiles for the peak temperatures in the throat-region and injector-end locations

In order to achieve a chamber design with a lower pressure drop, the same chamber was evaluated incorporating 150 cooling channels in the design. Although the channel width for the reduced number of channels is larger, the aspect ratio in the throat region was held at 6 by increasing the height of the channels relative to the 200 channel case. As in the previous cases, the chamber was first evaluated with unblocked channels. In this case, the pressure drop was 587 psi, which resulted in a lower coolant inlet pressure of 2900 psia.

Again, the peak wall temperature occurs just upstream of the throat at a value of 1211R, 153R higher than the 200 channel case. The temperature profile for this location is shown in Figure 12. The dashed line in Figure 13 shows the average hot-gas-side wall temperature as a function of axial position for the unblocked-channel case. This figure also shows the step changes in wall temperature just before and just after the step change in the cooling channel width in the nozzle and chamber respectively, at $x \approx 1.0$ inch and $x \approx 4.0$ inches.

The same high-pressure chamber was evaluated by running RTE with the blocked-channel option. In order to maintain the pressure drop of 587 psi for the cooling channel adjacent to the blocked channel, the mass flow rate of the coolant was reduced from 0.043 lb/sec per channel to 0.031 lb/sec per channel, a 28% reduction in the coolant mass flow. The resulting average hot-gas-side wall temperature as a function of axial position for the blocked-channel and adjacent open channel is also shown in Figure 13. A maximum wall temperature of 1766R for this case occurs just upstream of the throat and is shown in the temperature profile in Figure 14. At the injector end of the cooling channels the maximum wall temperature reached 1738R as shown in Figure 15.

The 150-channel design resulted in a conservative axial wall temperature profile with a reasonable pressure drop across the cooling jacket. However, the peak wall temperatures for the blocked-channel case are in a range where severe plastic deformation of the cooling channel on the hot-gas-side wall could occur.

SUMMARY AND CONCLUDING REMARKS

Rocket Thermal Evaluation (RTE) code was used to investigate the effects of a blocked channel on the wall temperature profile of three regeneratively cooled rocket thrust chambers, one at a low chamber pressure and two at a high chamber pressure. All three chambers incorporated HARRC in the designs, resulting in conservative wall temperature profiles when there was no channel blockage.

For the blocked channel cases, the analysis showed the effect on the wall temperature for the blocked channel and the adjacent open channel. The results indicated that there is a significant increase in the hot-gas-side wall temperature of the blocked channel and the adjacent open channel and a significant reduction in the coolant mass flow in the adjacent open channel. The increase in wall temperature due to a blocked channel for the low chamber pressure case was not at a level that would cause significant

wall damage. However, the peak wall temperatures in the blocked channels for the high chamber pressure cases were at levels that could result in severe plastic deformation occurring in the cooling channel hot-gas-side wall, especially for the 150 channel high-pressure chamber.

It should be noted, however, that none of the hot-gas-side wall temperatures in the blocked-channel and the adjacent open channel for the low- and high-pressure chambers were anywhere near the melting temperature of copper. This is another advantage of using high-conductivity materials in the design of rocket thrust chamber cooling jackets. It provides a margin of safety. If the cooling jacket in the main combustion chamber of a rocket engine were fabricated from stainless steel tubes, undoubtedly a blocked tube would result in a burnout of that tube and possibly cause a catastrophic failure of the chamber.

If this analysis had included two or more channels adjacent to the blocked channel, the resulting wall temperatures would have been somewhat lower. However, for this analysis, only the blocked channel and the adjacent open channel were considered, which is a worst case scenario.

REFERENCES

1. Mohammad H.N. Naraghi, "RTE – A Computer Code for Three-Dimensional Rocket Thermal Evaluation," <http://www.manhattan.edu/~mnaraghi/rte/rte.pdf>.
2. Mary F. Wadel, Richard J. Quentmeyer, and Michael L. Meyer, "A Rocket Engine Design for Validating the High-Aspect-Ratio Cooling Concept," Preprint from the 1994 Conference on Advanced Earth-To-Orbit Propulsion Technology held at NASA Marshall Space Flight Center, Huntsville, AL, May 17-19, 1994.
3. Mary F. Wadel and Michael L. Meyer, "Validation of High-Aspect-Ratio Cooling in a 89kN (20,000 lbf) Thrust Combustion Chamber," AIAA/ASME/SAE/ASEE 32nd Joint Propulsion Conference; July 1-3, 1996 / Lake Buena Vista, FL, AIAA-96-2584
4. S. Gordon and Bonnie J. McBride, "Computer Program for Calculation of complex Chemical Equilibrium Compositions, Rocket Performance,

- Incident and Reflection Shocks, and Chapman-Jouquet Detonations,” NASA SP-270, 1971.
5. S. Gordon, Bonnie J. McBride and F.J. Zeleznik, “Computer Program for Calculation of Complex Chemical Equilibrium Compositions and Applications Supplement I -Transport Properties,” NASA TM-86885, Oct. 1984.
 6. Robert C. Hendricks, A.K. Baron and I.C. Peller, “GASP - A Computer Code for Calculating the Thermodynamic and Transport Properties for Ten Fluids: Parahydrogen, Helium, Neon, Methane, Nitrogen, Carbon Monoxide, Oxygen, Fluorine, Argon, and Carbon Dioxide,” NASA TN D-7808, Feb. 1975.
 7. Robert C. Hendricks, I.C. Peller and A.K. Baron, “WASP - A Flexible Fortran IV Computer Code for Calculating Water and Steam Properties,” NASA TN D-7391, Nov, 1973.
 8. E. R. G. Eckert and R. M. Drake, “Analysis of Heat and Mass Transfer,” McGraw-Hill Book Company, 1972.
 9. D.R. Bartz, “Turbulent Boundary-Layer Heat Transfer from Rapidly Accelerating Flow of Rocket Combustion Gases and of Heated Air,” Advances in Heat Transfer, pp. 2-108, 1965.
 10. G.R. Nickerson, D.E. Coats, A.L. Dang, S.S. Dunn, and H. Kehtarnavaz, “Two-Dimensional Kinetics (TDK) Nozzle Performance Computer Program,” NAS8-36863, March 1989.
 11. Robert C. Hendricks, M. Niino, A. Kumakawa, V.M. Yernshenko, L.A. Yaski, L.A. Majumdar, and J. Mukerjee, “Friction Factors and Heat Transfer Coefficients for Hydrogen Systems Operating at Supercritical Pressures,” Proceeding of Beijing International Symposium on Hydrogen Systems, Beijing, China, May 7-11, 1985.
 12. A. Kumakawa, M. Niino, R.C. Hendricks, P.J. Giarratano, and V.D. Arp, “Volume-Energy Parameters for Heat Transfer to Supercritical Fluids,” Proceeding of the Fifteenth International Symposium of Space Technology and Science, Tokyo, pp. 389-399, 1986.
 13. A. Froehlich, H. Immich, F. LeBail, and M. Popp, “Three-Dimensional Flow Analysis in a Rocket Engine Coolant Channel of High Depth/Width Ratio,” AIAA/SAE/ASME/ASEE 27th Joint Propulsion Conference; June 24-26, 1991 / Sacramento, CA, AIAA-91-2183
 14. Julie A. Carlile and Richard J. Quentmeyer, “An Experimental Investigation of High-Aspect-Ratio Cooling Passages,” AIAA/SAE/ASME/ASEE 28th Joint Propulsion Conference; July 6-8, 1992 / Nashville, TN, AIAA-92-3154.
 15. Michael L. Meyer and James E. Giuliani, “Visualization of Secondary Flow Development in High-Aspect-Ratio Channels with Curvature”, AIAA/ASME/SAE/ASEE 30th Joint Propulsion Conference; June 27-29, 1994 / Indianapolis, IN, AIAA-94-2979.
 16. Michael L. Meyer, “Electrically Heated Tube Investigation of Cooling Channel Geometry Effects”, AIAA/SAE/ASME/ASEE 31st Joint Propulsion Conference, San Diego, CA, AIAA-95-2500.
 17. F. Neuner, D. Preclik, M. Popp, M. Funke, and H. Kluttig, “Experimental and Analytical Investigation of Local Heat Transfer in High-Aspect-Ratio Cooling Channels”, AIAA/ASME/SAE/ASEE 34th Joint Propulsion Conference; July 13-15, 1998 / Cleveland, OH, AIAA-98-3439

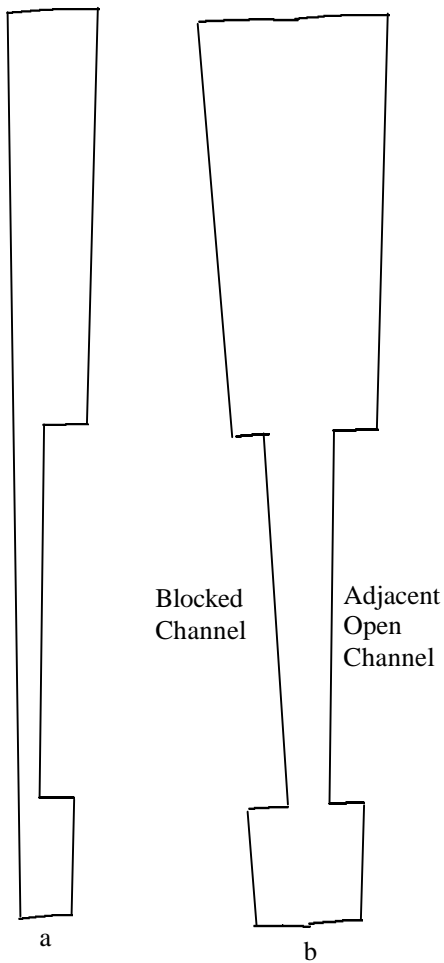


Figure 1: (a) One-half cooling channel and half-rib cross-section (b) One-half blocked channel and one-half open channel with full-rib.

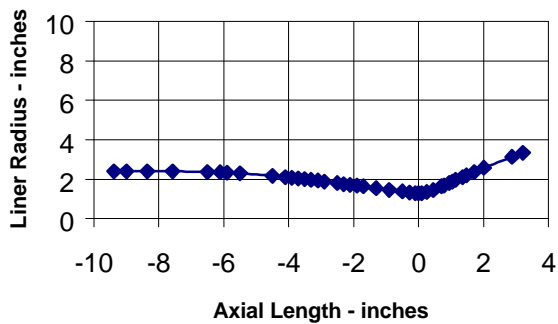


Figure 2: The high-pressure rocket thrust chamber contour showing station locations

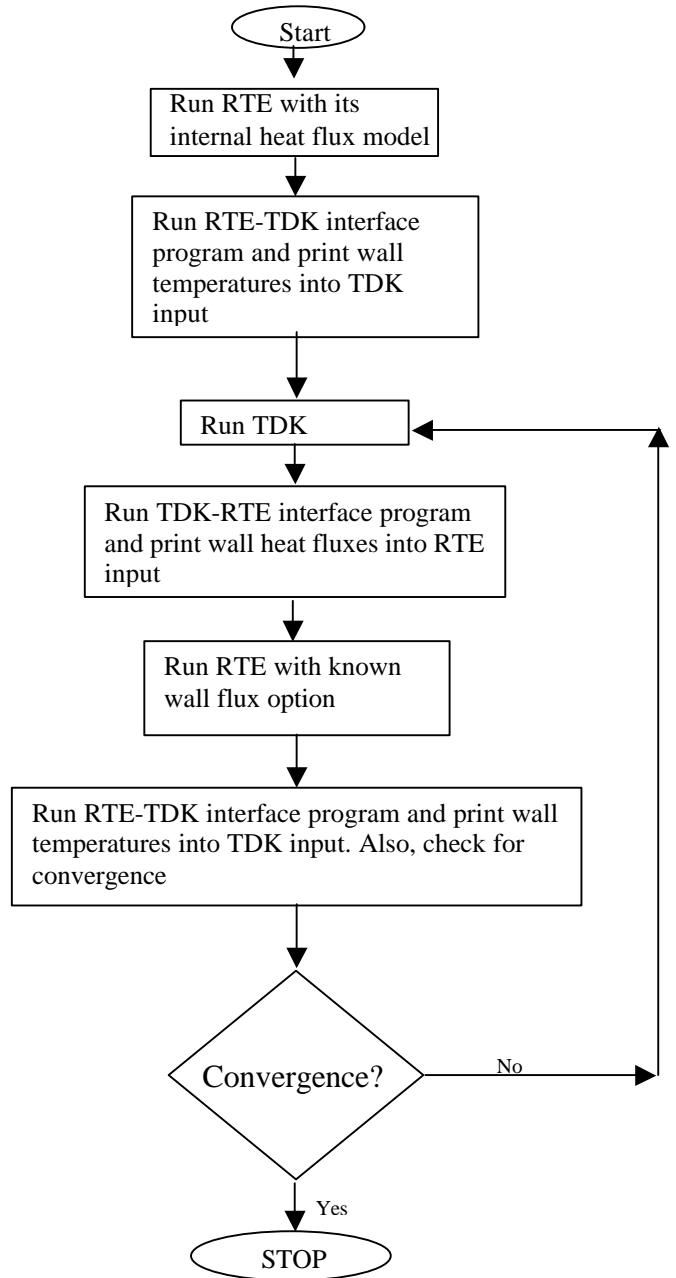


Figure 3: RTE and TDK interface

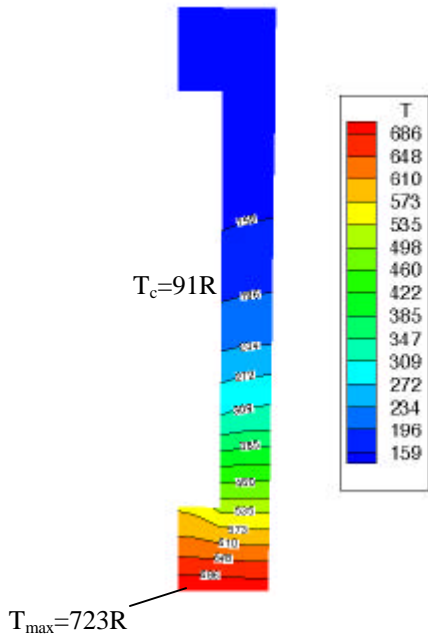


Figure 4: Rib temperature profile upstream of the throat ($x=-0.618$) for the low-pressure chamber, 240 channels (unblocked)

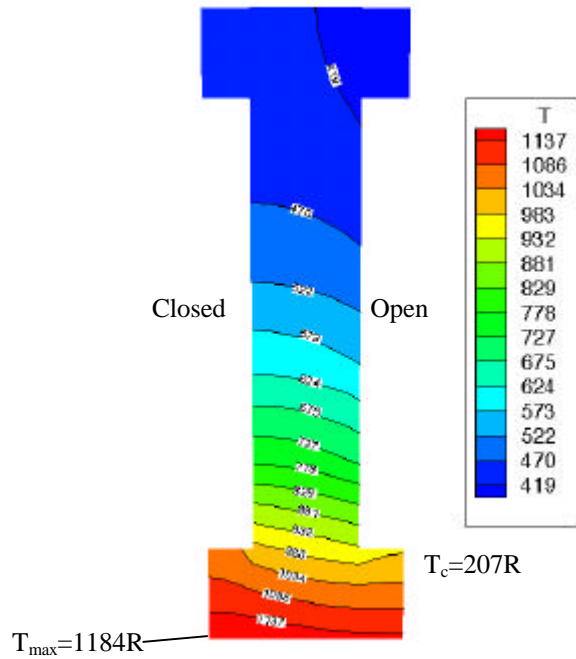


Figure 6: Rib temperature profile upstream of the throat ($x=-0.618$) for the low-pressure chamber, 240 channels (blocked channel and adjacent open channel)

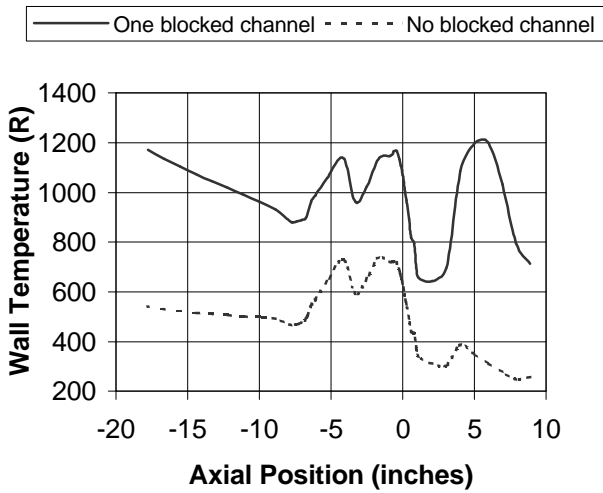


Figure 5: Comparison of the maximum wall temperature profile versus axial position for the blocked-channel profile and unblocked channel cases for the low-pressure chamber, 240 channels

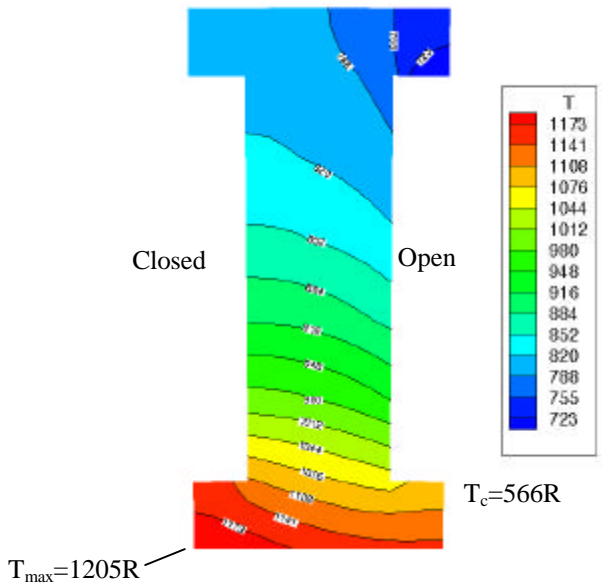


Figure 7: Rib temperature profile at the injector-end station ($x=-17.78$ inches) for the low-pressure chamber, 240 channels (blocked channel and adjacent open channel)

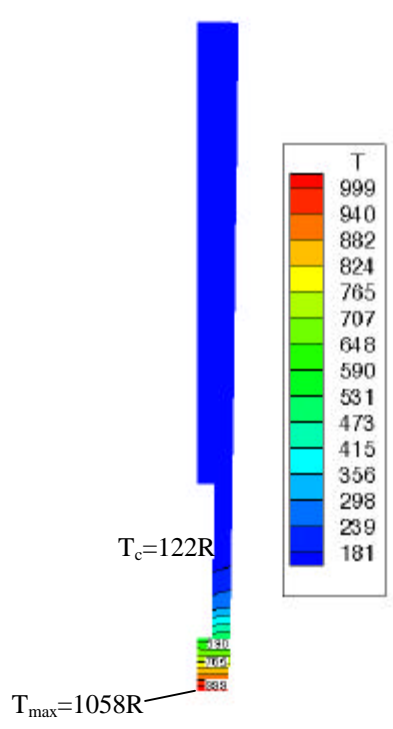


Figure 8: Rib temperature profile upstream of the throat ($x=-0.1$ inches) for the high-pressure chamber, 200 channels (unblocked)

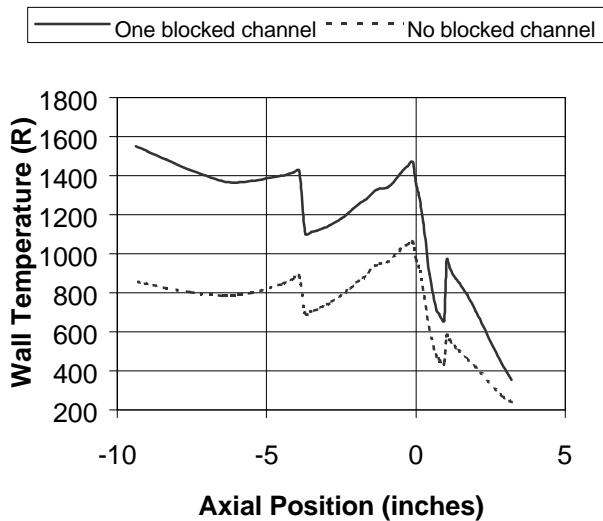


Figure 9: Comparison of the maximum wall temperature profile versus axial position for the blocked-channel and unblocked-channel cases for the high-pressure chamber, 200 channels

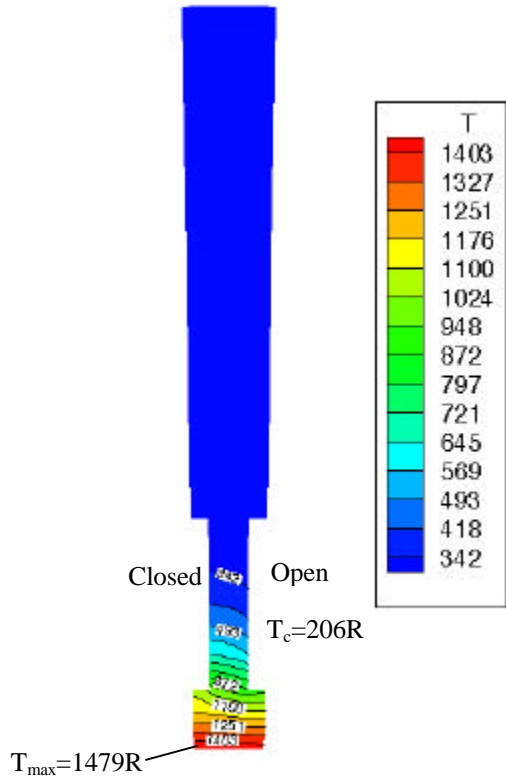


Figure 10: Rib temperature profile upstream of the throat ($x=-0.1$ inches) of the high-pressure chamber, 200 channels (blocked channel and adjacent open channel)

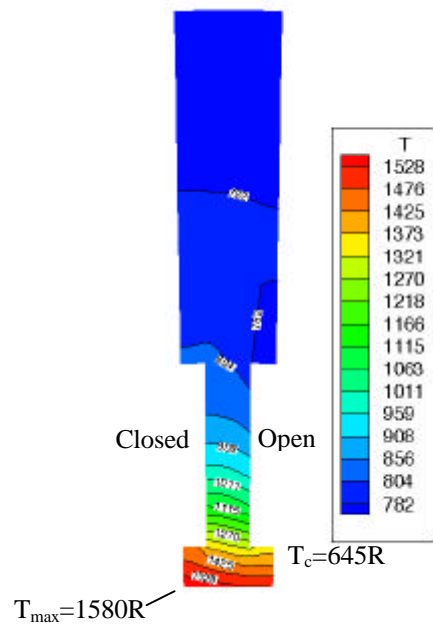


Figure 11: Rib temperature profile at the injector-end station ($x=-9.38$ inches) for the high-pressure chamber, 200 channels (blocked channel and adjacent open channel)

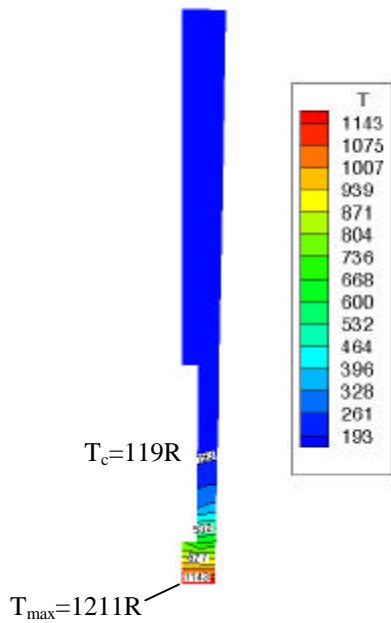


Figure 12: Rib temperature profile upstream of the throat ($x=-0.1$ inches) for the high-pressure chamber, 150 channels (unblocked)

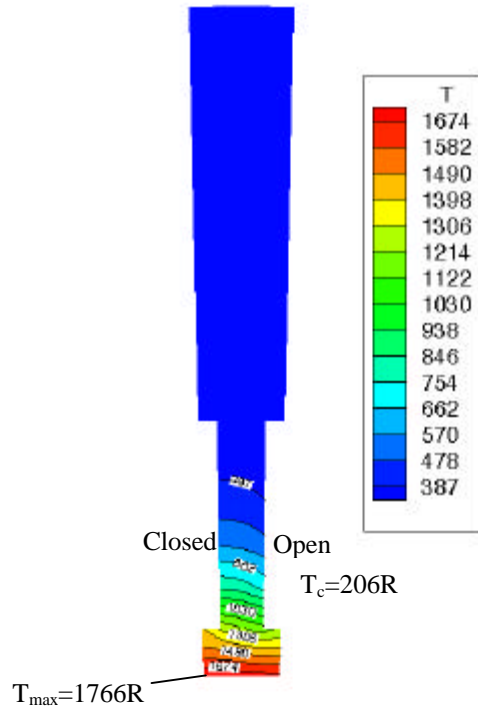


Figure 14: Rib temperature profile upstream of the throat ($x=-.01$ inches) for the high-pressure chamber, 150 channels (blocked channel and adjacent open channel)

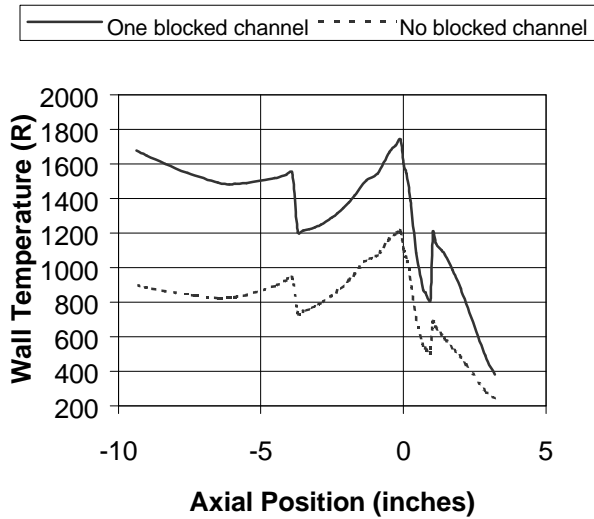


Figure 13: Comparison of the maximum wall temperature profile versus axial position for the blocked-channel and unblocked-channel cases for the high-pressure chamber, 150 channels

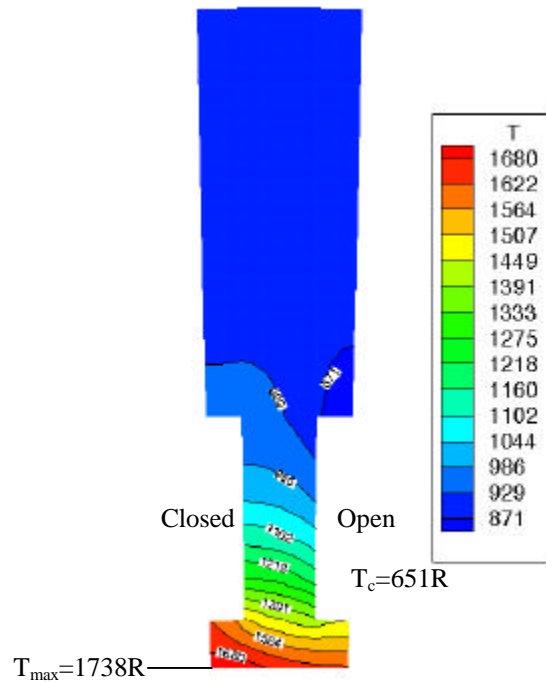


Figure 15: Rib temperature profile at the injector-end station ($x=-9.38$ inches) for the high-pressure chamber, 150 channels (blocked channel and adjacent open channel)